UDC: 616.65-006:073.756.8 DOI: 10.52532/2663-4864-2023-2-68-36-42

DWI CAPACITY IN PROSTATE CANCER DIAGNOSING

K.E. KARAKOISHIN[1], Zh.Zh. ZHOLDYBAY[1], A.S. AYNAKULOVA[1], D.K. TOLESHBAEV[1], G.M. MUHIT[1], YE. AYSERBAY[1]

[1]«Asfendiyarov Kazakh National Medical University» NCJSC, Almaty, the Republic of Kazakhstan

ABSTRACT

Relevance: *Prostate cancer is one of the leading causes of cancer deaths in men worldwide. Transrectal ultrasound-guided (TRUS) prostate biopsy is the most important diagnostic step, without which a definitive diagnosis cannot be made. Despite this, TRUS-guided prostate biopsy has a high rate of false negatives and is often accompanied by various clinical complications. Multiparametric MRI (mpMRI) is now widely used in routine urological and oncological practice. An element of mpMRI is diffusion-weighted imaging (DWI), which is successfully used in detecting and localizing clinically significant prostate cancer.*

The study aimed to *evaluate the DWI capacity in diagnosing prostate cancer.*

Methods: *52 patients, 48-86 years old, with suspected prostate cancer, underwent mpMRI. DWI sequences obtained using T2-weighted imaging (T2WI) were compared with each other and compared with the anatomical structure of the prostate. Suspicious prostate cancer sites were marked as regions of interest, for which an apparent diffusion coefficient (ADC) was calculated. A 12-point TRUS-guided biopsy confirmed the presence or absence of prostate cancer.*

Results: *When analyzing quantitative measurements, ADC showed low values for cancer in the cen-tral gland (transitional zone and central zone) – 0.610±0.157×10^{-3} mm^2/s, p=0.0001, and for cancer in the peripheral zone – 0.651±0.228×10^{-3} mm^2/s, p=0.0004, compared to normal tissue. It was found that the highest sensitivity value (87.5%) is typical for ADC central gland, and the lower value for ADC peripheral zone is 75%. The highest specificity value (90.9%) was observed in ADC peripheral zone, and a lower value in ADC central gland – was 84.1%.*

Conclusion: *DWI is an effective non-invasive method for detecting and localizing prostate cancer, providing a qualitative (visual) and quantitative assessment of prostate cancer.*

Keywords: *prostate cancer, multiparametric magnetic resonance imaging (mpMRI), transrectal ultrasound (TRUS), diffusion-weighted imaging (DWI).*

Introduction: Prostate cancer has a high prevalence and is one of the main causes of death of men from oncological diseases worldwide [1]. The problem of early diagnosis of prostate cancer is associated not only with the late treatment of patients but also with the insufficient accuracy of traditional diagnostic methods. The complexity of visualization of tumor foci in the prostate gland (PG) remains an urgent task, despite the modern development of prostate imaging methods. Ultrasound-guided transrectal biopsy of the prostate (TRUS) is the most important diagnostic step, without which it is impossible to make a final diagnosis. Despite this, TRUS-guided prostate biopsy has a high false-negative rate [2] and is often accompanied by various clinical complications [3]. Multiparametric MRI (mpMRI) is widely used in everyday urological and oncological practice. One of the elements of multiparametric MRI is diffusion-weighted imaging (DWI) [4, 5], which is successfully used in the detection and localization of clinically significant prostate cancer [6].

The study aimed to evaluate the DWI capacity in diagnosing prostate cancer.

Materials and methods:

Patients. The study protocol was developed based on the Sunkar Diagnostic and Treatment Center in Almaty, Kazakhstan. We selected 52 prostate cancer suspects aged 48-86 years. The inclusion criteria for the study were: an elevated PSA level and the patient's ability to give informed consent. The exclusion criteria were: contraindications for MRI and inability to decide and/or sign an informed consent sheet.

The mean age of the patients was 65.5 years (interquartile interval: 60.0-71.75), the mean PSA level was 9.5 (interquartile interval: 6.3-9.8 ng/mL), the mean prostate volume was 47, 5 (interquartile interval: 26.75-53.75). All patients underwent TRUS-guided biopsy. Prostate cancer was diagnosed in 8 patients; of them, four (7.7%) had a Gleason score of 7, two (3.8%) scored 8, one (1.9%) scored 6, and another one (1.9%) scored 9 (Table 1).

Table 1 – Characteristics of the study patients

	All (n=52)	Healthy controls, n=44	Prostate cancer patients, n=8	Significance
Age, average [IQR]	65.5 [60.0-71.75]	65.2 [58.25-71.0]	67.3 [63.0-72.0]	p=0.19
PSA (ng/ml), average [IQR]	9.5 [6.3-9.8]	8.1 [6.2-9.5]	17.2 [8.0-17.5]	p=0.08
Prostate volume on MRI (ml), average [IQR]	47.5 [26.75-53.75]	46.1 [25.25-61.0]	55.6 [37.75-53.75]	p=0.23

Table 1 (continued)

Gleason score	Value (%)
Gleason 6 (3 + 3)	1 (12.5%)
Gleason 7 (3 + 4)	4 (50.0%)
Gleason 7 (4 + 3)	0
Gleason 8 (4 + 4)	2 (25.0%)
Gleason 9 (4 + 5)	1 (12.5%)
Localization	n (%)
Cancer in the peripheral zone	3 (37.5%)
Cancer in the central gland	4 (50.0%)
Cancer in the central gland and peripheral zone	1 (12.5%)

Notes: n – number, PSA – prostate-specific antigen, IQR - interquartile range

MRI study protocol. mpMRI was performed on a 3T scanner (Signa Architect, GE, USA) with a surface coil. The data collection protocol included the following sequences:

1. Axial T2-weighted turbo spin echo sequence with fast relaxation T2WI frFSE (TR/TE – 4249/102.7 ms, slice thickness – 4 mm, gap – 0.5 mm, matrix – 352x288 mm, rotation angle (FLIP) – 111°, the number of averages (NEX) – 1, scan time – 2:52 min);

2. Sagittal T2-weighted turbo spin echo sequence with periodically rotated overlapping parallel lines with improved T2WI Propeller reconstruction (TR/TE – 10490/86.0 ms, slice thickness – 4 mm, gap – 0.4 mm, matrix – 320x320 mm, FLIP – 160°, NEX – 2.05, scan time – 5:53 min);

3. Axial T1-weighted turbo spin echo sequence with fat suppression T1WI FSEFS (TR / TE – 751/9.2 ms, slice thickness – 4 mm, gap – 0.5 mm, matrix – 384x224 mm, FLIP – 111°, NEX – 1, scan time – 3:59 min);

4. Coronal T2-weighted turbo spin echo sequence with fast relaxation T2WI frFSE (TR/TE – 5253/102.0 ms, slice thickness – 4 mm, gap – 0.5 mm, matrix – 412x320 mm, FLIP – 160°, NEX – 2, scan time – 4:55 min);

5. Coronal T1-weighted sequence of turbo spin echo T2WI FSE (TR/TE – 693/8.5 ms, slice thickness – 4 mm, gap – 0.5 mm, matrix – 320x320 mm, FLIP – 111°, NEX – 0.5, scan time – 1:55 min);

6. Diffusion-weighted sequence using a single DWI echo-planar sequence (TR/TE – 5400/75.3 ms, slice thickness – 4 mm, gap – 0.5 mm, matrix – 120x120 mm, 3*b*-values – 50, 600, 1000 s/mm^2, FLIP – 90°, NEX – 2, scan time – 3:57 min).

ADC Quantitative Maps. The anatomical structure of the prostate obtained using T2-weighted imaging (T2WI) was compared with DWI data and a map of the measured diffusion coefficient (apparent diffusion coefficient, ADC) obtained from DWI. Regions of interest were manually marked corresponding to cancer-suspicious sites in the central gland (central/transitional zones) and the peripheral zone of the prostate. The remaining sections of the prostate's central/transitional and peripheral zones were considered healthy areas (Figure 1). The average diffusion coefficient on the ADC was measured using the software Volume Viewer (GE, USA) at the workstation (GE) in the regions of interest.

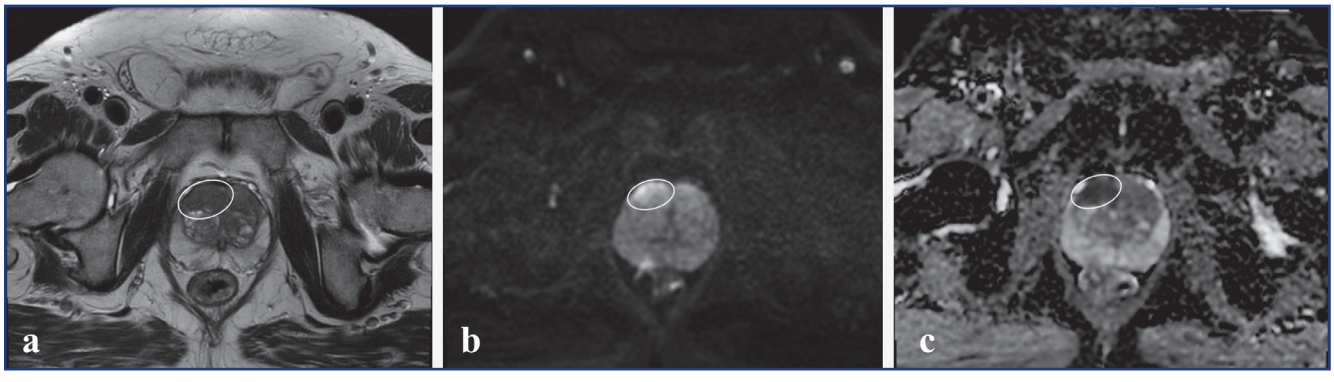

Picture 1 - Education in the central gland prostate: a – T2, b – DWI, c – ADC; white ellipsoid – prostate formation

Pathology. A TRUS-guided 12-point biopsy confirmed the presence or absence of prostate cancer.

Statistical analysis. Microsoft Excel and the IBM SPSS Statistics package served as a tool for the statistical processing of the obtained data. We used Student's t-test to evaluate differences in clinical scores and ADC values between normal tissue and cancerous lesions. Combined data on the results of diagnostic tests and data on the presence of prostate cancer confirmed by biopsy

and the results of association statistics: Fischer's Exact test and odds ratio were used. We calculated the ADC sensitivity and specificity in prostate cancer diagnostics. ADC ROC curve analysis was performed, and the area under the curve (AUC) was calculated.

Results: When analyzing quantitative measurements, ADC showed low values for cancer in the central gland (transition zone and central zone) – 0.610±0.157 (mean value ± SD)×10^{-3} mm^2/s, p=0.0001 and for cancer in the peripheral zone – 0.651±0.228 (mean value ± SD)×10^{-3} mm^2/s, p=0.0004, compared with normal tissue (table 2).

Table 2 – DWI values: ADC in the peripheral zone and central gland (transitional/central zones)

Values (10^{-3} mm^2/s)	Normal tissue	Prostate cancer	Average difference	Significance
Peripheral zone	1.279±0.457	0.651±0.228	-0.628	0.0004
Central gland	0.885±0.173	0.610±0.157	0.610	0.0001

Note: Data are presented as mean value ± standard deviation

When the ADC value in the identified cases of prostate cancer is correlated with the Gleason scale, lower ADC values (0.375×10^{-3} mm^2/s and 0.498×10^{-3} mm^2/s) correspond to the sum of Gleason scores of 9 and 8 (Table 3), which indicates a proportional relationship between ADC values and tumor aggressiveness.

Table 3 – ADC correlation with the Gleason score in post-biopsy patients

Central gland ADC (10^{-3} mm^2/s)	**Peripheral zone** ADC (10^{-3} mm^2/s)	**Gleason score**
0.685	0.692	7(3+4)
0.550	0.550	7(3+4)
0.570	0.590	7(3+4)
0.498	0.498	8(4+4)
0.912	0.935	7(3+4)
0.626	1.044	6(3+3)
0.665	0.525	8(4+4)
0.375	0.375	9(4+5)

Table 4 presents the combined data on the results of diagnostic tests and data on biopsy-confirmed prostate cancer, as well as the results of association statistics: Fischer's Exact test and odds ratio. Based on the analysis results, a statistically significant relationship/dependence was revealed between the diagnostic ability of the ADC of the central gland and the peripheral zone to correctly determine the presence of prostate cancer in patients. Fischer's Exact test statistic was considered significant at p<0.001.

Table 4 – Baseline test results vs. biopsy-confirmed prostate cancer and association statistics

Diagnostic tests	prostate cancer		Fischer's Exact test (FET)	Odds ratio
	+	–		
Diagnosis of ADC (central gland)				
Below 0.700×10^{-3} mm^2/s	7	7	FET=0.00018, p<0.001	37.000
Over 0.700×10^{-3} mm^2/s	1	37		
ADC diagnostics (peripheral zone)				
Below 0.700×10^{-3} mm^2/s	6	4	FET=0.00025, p<0.001	30.000
Over 0.700×10^{-3} mm^2/s	2	40		

The obtained results indicate that the ADCs of the central gland below the threshold of 0.700×10^{-3} mm^2/s increase the chance of clinical verification of prostate cancer by 37 times, and the peripheral zone ADC values below 0.700×10^{-3} mm^2/s increase the prostate cancer probability 30 times.

Table 5 presents the ADC sensitivity and specificity in diagnosing prostate cancer. The highest sensitivity of 87.5% was typical for the central gland's ADC, and the peripheral zone's ADC had a lower sensitivity of 75%. ADC of the peripheral zone had the highest specificity of 90.9%, and the ADC of the central gland had a lower specificity of 84.1%.

Table 5 – ADC sensitivity and specificity in prostate cancer diagnosing

Diagnostic tests	Sensitivity	Specificity
ADC (central and transitory zone)	0.875	0.841
ADC (peripheral zone)	0.750	0.909

Along with determining sensitivity and specificity values, plots of sensitivity versus specificity were plotted. Figure 2 shows the ROC curves of the diagnostic ability of the logistic regression model for adenocarcinoma verification.

The constructed curves for the central gland and the peripheral zone ADCs mostly located in the upper left corner of the graph, indicating acceptable diagnostic properties of the tests.

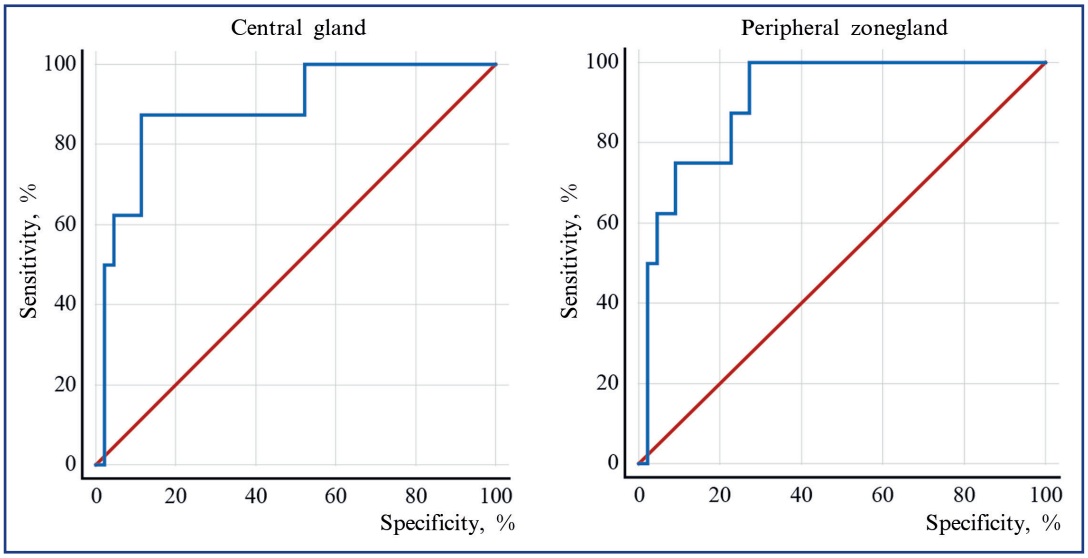

Figure 2 – ROC curves of diagnostic ability of the logistic regression model of prostate cancer verification

At the final stage, the area under the ROC curves was estimated (Table 6).

Table 6 – Area under the ROC curve

Diagnostic tests	Area [CI]	Asymptotic Significance
ADC (central gland)	0.889 [0.733÷1.000]	p=0.001
ADC (peripheral zone)	0.909 [0.820÷0.998]	p<0.001

In the study, ADC showed high diagnostic accuracy, with an area of -0.909 for the peripheral zone and -0.889 for the central gland. Both tests are characterized by high (excellent) quality predictive accuracy.

Discussion: Diffusion is a physiological process of random thermal movement of water molecules in tissues. Visualization of the DWI image is determined by the difference in the speed of movement of water molecules in different biological tissues, and this movement is inversely proportional to the cellularity of the tissue and the integrity of the cell membrane. Therefore, diffusion capacity is retained in normal tissue, resulting in low signal intensity on DWI. Tumor formation destroys the normal tissue structure and has a higher cell density than normal tissue. Therefore, in the cancerous tissue, the movement of water molecules is limited, resulting in high signal intensity on DWI. In addition, using DWI, differences in the movement of water molecules are qualitatively assessed by the relative intensity of the tissue signal but can also be assessed quantitatively by calculating the ADC [7].

In everyday clinical practice, an MRI of the prostate is performed using 1.5- or 3 T-tomographs using a multichannel surface coil for the trunk or endorectal coil. The endorectal coil increases the signal-to-noise ratio (SNR) of an MR image, but high examination cost, patient discomfort, and susceptibility artifacts limit its use [5]. DWI is usually performed in the axial plane using single or multiple EPI planar echo imaging. In particular, single EPI is sensitive to motion and susceptibility artifacts to any metal inserts in the body or air in the rectum. For DWI of the prostate, B values from 50 to 1400 s/mm^2 on a 1.5 T tomograph and from 1000 to 2000 s/mm^2 on a 3 T tomograph are commonly used [5]. In our study, we performed DWI on a 3 T MRI using a single echo-planar sequence and a surface coil.

In earlier studies, using a 1.5 T tomograph, ADC values in normal prostate tissues were as follows: in the peripheral zone of the prostate – 1.0-1.9×10^{-3} mm^2/s; in the central gland of the prostate (central and transient zone) – 0.9-1.7×10^{-3} mm^2/s. When using a 3.0 T tomograph, the ADC values in normal tissues of the prostate were as follows: in the peripheral zone of the prostate – 0.8-2.6×10^{-3} mm^2/s; in the central gland of the prostate (central and transient zone) – 0.8-2.2×10^{-3} mm^2/s. ADC values tended to be higher in the peripheral zone than in the central gland and higher with the 3.0 T scanner than the 1.5 T scanner [7].

The values of ADC in malignant lesions of the prostate using a 1.5 T tomograph were as follows: in the pe-

ripheral zone – 0.6-1.4×10^{-3} mm^2/s; in the central gland – 0.9-1.1×10^{-3} mm^2/s; when using a 3.0 T tomograph: in the peripheral zone – 0.6-1.6×10^{-3} mm^2/s, in the central gland – 0.8-1.6×10^{-3} mm^2/s. Therefore, the ADC values in the peripheral zone and the central gland were almost identical but tended to increase when using a 3.0 T tomograph. In addition, in all studies conducted, ADC values in malignant lesions of the peripheral zone and central gland were lower than the normal prostate's corresponding areas. Moreover, at higher b values, ADC values in normal and cancerous tissues tended to decrease [7].

In our study using a 3.0 T tomograph, in normal tissues of the prostate, there was also an increase in the ADC value in the peripheral zone (1.279±0.457×10^{-3} mm^2/s, mean ± SD) compared with the central gland (0.885.25±0.173×10^{-3} mm^2/s, mean ± SD). ADC values in cancer-suspicious areas were lower compared to normal prostate tissue both in the peripheral zone (0.651±0.228×10^{-3} mm^2/s, mean ± SD) and in the central gland (0.610±0.157×10^{-3} mm^2/s, mean ± SD).

However, ADC values can often be the same in normal and cancerous tissues. Some studies have reported limitations in differentiating normal tissue from malignant lesions. In particular, the use of ADC threshold values of 1.67×10^{-3} mm^2/s for the peripheral zone and 1.61×10^{-3} mm^2/s for the central gland on a 1.5 T tomograph gives good results in detecting prostate cancer with sensitivity and specificity of 94% and 91% for the peripheral zone and 90% and 84% for the central gland. The use of the ADC threshold value of 1.35×10^{-3} mm^2/s demonstrates the sensitivity and specificity of ADC in detecting prostate cancer – 88% and 96%, respectively, both in the peripheral zone and the central gland [7]. Therefore, differences in magnetic field strength affect the accuracy of prostate cancer diagnosis. In addition, ADC measurement is particularly useful for improving the detection of central cancer (central and transient zone), as there are significant differences in ADC values in central cancer, stromal hyperplasia, and glandular hyperplasia [5, 8].

In our study, we used ADC threshold values for the peripheral zone and central gland – 0.700×10^{-3} mm^2/s, while the sensitivity and specificity of prostate cancer diagnosis for the peripheral zone were 75% and 90.9%, respectively, and for the central gland – 87.5% and 84.1%, respectively. The results obtained are comparatively lower than previous studies, which is more likely due to the low threshold value of ADC and the small number of patients.

In recent studies, prostate cancer detection sensitivity on T2WI was 54-96%, with a specificity of 21-91%, but the results varied between studies. The low specificity of T2WI has also been reported. DWI has a relatively high specificity, and when DWI is combined with T2WI, sensitivity and area under the ROC curve increase [7, 8].

Our study compared T2WI and DWI, followed by the ADC measurement in cancer-suspicious prostate areas, and showed high diagnostic accuracy, with a ROC curve area of 0.909 for the peripheral zone and 0.889 for the central gland.

Compared to T2WI and DCE, DWI is the most effective and the only sequence for detecting prostate cancer [5]. The combination of DWI and T2WI – biparametric MRI (bpMRI) – increases the sensitivity of diagnosing prostate cancer of both the central gland and the peripheral zone [9-14]. However, bpMRI provides a lower prostate cancer diagnosing accuracy compared to the combined use of T2WI, DWI, and DCE (mpMRI) [10, 14].

Higher *b*-values may increase diffusion weighting, contrast-to-noise ratio (CNR), and theoretically better prostate cancer detection. The disadvantages are the frequent appearance of motion and susceptibility artifacts and a reduced SNR [7]. Koo et al. compared b=1000 s/mm^2 and b=2000 s/mm^2 and reported that b=1000 s/mm^2 had a higher ADC sensitivity in detecting prostate cancer, but the specificity at b=1000 s/mm^2 was lower compared to b=2000 s/mm^2 [15]. After qualitatively evaluating the DWI image, Rosenkrantz et al. and Ueno et al. showed that b=2000 s/mm^2 is preferable for diagnosing prostate cancer compared to b=1000 s/mm^2 [16, 17]. When evaluating ADC maps in the diagnosis of prostate cancer, Rosenkrantz et al. found no significant difference between b=1000 s/mm^2 and b=2000 s/mm^2 [16]. In a qualitative DWI image analysis, Manenti et al. reported a higher sensitivity of b=2000 s/mm^2 than b=1000 s/mm^2 in diagnosing prostate cancer for less and more experienced radiologists. In their opinion, images with a value of b=1000 s/mm^2 cannot suppress benign prostate tissue and sometimes hide tumor lesions. Regarding the quantification of ADC maps, a higher diagnostic accuracy was obtained at b=2000 s/mm^2 compared to b=1000 s/mm^2, although this was not statistically significant [18].

In our study using a 3 T tomograph, we applied b = 50, 600, and 1000 s/mm^2 and obtained a good SNR and a few motion or susceptibility artifacts. At the same time, the signal intensity in the cancerous areas on DWI was increased, while in the surrounding normal areas, it decreased (Fig. 1).

Assessment of tumor aggressiveness with ADC is currently an area of clinical application of DWI that is attracting much attention. According to some authors, ADC can serve as a potential marker of PCa aggressiveness and a prognostic indicator [7]. Several investigators have reported that ADC can detect high-risk cancers with a Gleason score of ≥7 [19, 20]. While previous studies have shown the importance of using ADC with a high b value for differentiating a non-cancerous lesion from prostate cancer, in the study by Barbieri et al., these parameters were found to provide little additional information when correlating high and low grade formation. They reported that ADC values differ between high-grade and low-grade prostate cancer, but given the large overlap in ADC values between high- and low-grade

prostate cancer, non-invasive diagnosis of individual patients using DWI in clinical practice is not yet possible [21].

We correlated the ADC value in identified cases of prostate cancer with the Gleason score and found that lower ADC values (0.375×10^{-3} mm^2/s and 0.498×10^{-3} mm^2/s) to the Gleason scores of 9 and 8, indicating a proportional relationship between the ADC value and the tumor aggressiveness.

Our study demonstrates high diagnostic accuracy DWI using a 3.0 T tomograph, with *b*-values = 50, 600, 1000 s/mm^2, ADC threshold for the peripheral zone and central gland – 0.700×10^{-3} mm^2/s in the diagnosis of prostate cancer.

Conclusion: DWI is an effective non-invasive method for diagnosing and localizing prostate cancer, providing a qualitative (visual) and quantitative assessment of prostate cancer.

References:

1. Sung H., Ferlay J., Siegel RL, Laversanne M., Soerjomataram I., Jemal A., Bray F. Global Cancer Statistics 2020: GLOBOCAN Estimates of Incidence and Mortality Worldwide for 36 Cancers in 185 Countries // CA Cancer J. Clin. – 2021. – Vol.71, No. 3. – P 209-249. https://doi.org/10.3322/caac.21660

2. Richenberg J., Løgager V., Panebianco V., Rouviere O., Villeirs G., Schoots IG The primacy of multiparametric MRI in men with suspected prostate cancer // Eur. Radiol. – 2019. - Vol. 29(12). – P. 6940-6952. https://doi.org/10.1007/s00330-019-06166-z

3. Borghesi M., Ahmed H., Nam R., Schaeffer E., Schiavina R., Taneja S., Loeb S. Complications After Systematic, Random, and Image-guided Prostate Biopsy // Eur. Urol. – 2017. – Vol. 71(3). – P. 353-365. https://doi.org/10.1016/j.eururo.2016.08.004

4. Hamoen E.H.J., de Rooij M., Witjes J.A., Barentsz J.O., Rovers M.M. Use of the Prostate Imaging Reporting and Data System (PI-RADS) for Prostate Cancer Detection with Multiparametric Magnetic Resonance Imaging: A Diagnostic Meta-analysis // Eur. Urol. – 2015. – Vol. 67(6). – P. 1112-1121. https://doi.org/10.1016/j.eururo.2014.10.033

5. Weinreb J.C., Barentsz J.O., Choyke P.L., Cornud F., Haider M.A., Macura K.J., Verma S. PI-RADS Prostate Imaging – Reporting and Data System: 2015, Version 2 // Eur. Urol. – 2016. - Vol. 69(1). – P. 16-40. https://doi.org/10.1016/j.eururo.2015.08.052

6. Tamada T., Kido A., Yamamoto A., Takeuchi M., Miyaji Y., Moriya T., Sone T. Comparison of Biparametric and Multiparametric MRI for Clinically Significant Prostate Cancer Detection With PI-RADS Version 2.1 // JMRI. - 2021. - Vol. 53(1). – P. 283-291. https://doi.org/10.1002/jmri.27283

7. Tamada T., Sone T., Jo Y., Yamamoto A., Ito K. Diffusion-weighted MRI and its role in prostate cancer // NMR Biomed. – 2013. – Vol. 27(1). – P. 25-38. https://doi.org/10.1002/nbm.2956

8. Stabile A., Giganti F., Rosenkrantz AB, Taneja SS, Villeirs G., Gill IS, Kasivisvanathan V. Multiparametric MRI for prostate cancer diagnosis: current status and future directions // Nat. Rev. Urol. – 2020. – Vol. 17(1). – P. 41-61. https://doi.org/10.1038/s41585-019-0212-4

9. Alabousi M., Salameh J.P., Gusenbauer K., Samoilov L., Jafri A., Yu H., Alabousi A. Biparametric versus Multiparametric Prostate MRI for the Detection of Prostate Cancer in Treatment-Naive Patients: A Diagnostic Test Accuracy Systematic Review and Meta-Analysis // BJU Int. – 2019. – Vol. 124(2). – P. 209-220. https://doi.org/10.1111/bju.14759

10. Niu X., Chen X., Chen Z., Chen L., Li J., Peng T. Diagnostic Performance of Biparametric MRI for Detection of Prostate Cancer: A Systematic Review and Meta-Analysis // Am. J. Roentgenol. – 2018. – Vol. 211(2). - P. 369-378. https://doi.org/10.2214/ajr.17.18946

11. Woo S., Suh C.H., Kim S.Y., Cho J.Y., Kim S.H., Moon M.H. Head-to-Head Comparison Between Biparametric and Multiparametric MRI for the Diagnosis of Prostate Cancer: A Systematic Review and Meta-Analysis // Am. J. Roentgenol. – 2018. – Vol. 211(5). – P. W226-W241. https://doi.org/10.2214/ajr.18.19880

12. Kang Z., Min X., Weinreb J., Li Q., Feng Z., Wang L. Abbreviated Biparametric Versus Standard Multiparametric MRI for Diagnosis of Prostate Cancer: A Systematic Review and Meta-Analysis // Am. J. Roentgenol. – 2019. – Vol. 212(2). – P. 357-365. https://doi.org/10.2214/ajr.18.20103

13. Monni F., Fontanella P., Grasso A., Wiklund P., Ou Y.C., Randazzo M., Bianchi G. Magnetic resonance imaging in prostate cancer detection and management: a systematic review // Minerva Urol. Nephrol. – 2017. – Vol. 69(6). – P.567–578. https://doi.org/10.23736/s0393-2249.17.02819-3

14. Xu L., Zhang G., Shi B., Liu Y., Zou T., Yan W., Sun H. Comparison of biparametric and multiparametric MRI in the diagnosis of prostate cancer // Cancer Imaging – 2019. – Vol. 19(1). – Art. no. 90. https://doi.org/10.1186/s40644-019-0274-9

15. Koo J.H., Kim C.K., Choi D., Park B.K., Kwon G.Y., Kim B. Diffusion-Weighted Magnetic Resonance Imaging for the Evaluation of Prostate Cancer: Optimal B Value at 3T // Korean J. Radiol. – 2013. – Vol. 14(1). – P. 61-69. https://doi.org/10.3348/kjr.2013.14.1.61

16. Rosenkrantz AB, Hindman N., Lim R.P., Das K., Babb J.S., Mussi T.C., Taneja S.S. Diffusion-weighted imaging of the prostate: Comparison of b1000 and b2000 image sets for index lesion detection // JMRI. – 2013. – Vol. 38(3). – P. 694-700. https://doi.org/10.1002/jmri.24016

17. Ueno Y., Takahashi S., Kitajima K., Kimura T., Aoki I., Kawakami F., Sugimura K. Computed diffusion-weighted imaging using 3-T magnetic resonance imaging for prostate cancer diagnosis // Eur. Radiol. – 2013. – Vol. 23(12). – P. 3509-3516. https://doi.org/10.1007/s00330-013-2958-z

18. Manenti G., Nezzo M., Chegai F., Vasili E., Bonanno E., Simonetti G. DWI of prostate Optimal b-Value in Clinical Practice // Prostate Cancer. – 2014. – Vol. 2014. – P. 1-9. https://doi.org/10.1155/2014/868269

19. Bratan F., Niaf E., Melodelima C., Chesnais AL, Souchon R., Mège-Lechevallier F., Rouvière, O. Influence of imaging and histological factors on prostate cancer detection and localization on multiparametric MRI: a prospective study // Eur. Radiol. – 2013. – Vol. 23(7). – P. 2019-2029. https://doi.org/10.1007/s00330-013-2795-0

20. Le J.D., Tan N., Shkolyar E., Lu D.Y., Kwan L., Marks L.S., Reiter R.E. Multifocality and Prostate Cancer Detection by Multiparametric Magnetic Resonance Imaging: Correlation with Whole-mount Histopathology // Eur. Urol. – 2015. – Vol. 67(3). – P. 569-576. https://doi.org/10.1016/j.eururo.2014.08.079

21. Barbieri S., Brönnimann M., Boxler S., Vermathen P., Thoeny HC Differentiation of prostate cancer lesions with high and with low Gleason score by diffusion-weighted MRI // Eur. Radiol. – 2017. – Vol. 27(4). – P. 1547-1555. https://doi.org/10.1007/s00330-016-4449-5

АНДАТПА

ҚУЫҚ АСТЫ БЕЗІНІҢ ҚАТЕРЛІ ІСІГІН ДИАГНОСТИКАЛАУДАҒЫ DWI-дың МҮМКІНДІКТЕРІ

К.Е. Каракойшин[1], Ж.Ж. Жолдыбай[1], А.С. Айнакулова[1], Д.К. Толешбаев[1], Г.М. Мухит[1], Е. Айсербай[1]

[1]«С.Д. Асфендияров атындағы Қазақ Ұлттық Медицина Университеті» КЕАҚ, Алматы, Қазақстан Республикасы

Өзектілігі: *Қуық асты безінің қатерлі ісігі бүкіл әлем бойынша ерлер арасындағы қатерлі ісік өлімінің негізгі себептерінің бірі болып табылады. УДЗ жетекшілігімен қуық асты безінің трансректалды биопсиясы диагностикалық маңызды қадам болып табылады, онсыз соңғы диагнозды қою мүмкін емес. Осыған қарамастан, УДЗ басқаратын қуық асты безінің биопсиясы жоғары жалған-теріс көрсеткішке ие және жиі әртүрлі клиникалық асқынулармен байланысты. Көппараметрлі МРТ қазіргі уақытта күнделікті урологиялық және онкологиялық тәжірибеде белсенді түрде қолданылады. Көппараметрлі МРТ элементтерінің бірі простата безінің клиникалық маңызды обырын анықтауда және локализациялауда сәтті қолданылған диффузиялық өлшенген бейнелеу (DWI) болып табылады.*

Зерттеудің мақсаты *– қуық асты безінің қатерлі ісігін диагностикалауда DWI мүмкіндіктерін бағалау.*

Әдістері: *48-86 жас аралығындағы қуық асты безінің обырына күдікті 52 пациентке көппараметрлік МРТ, соның ішінде DWI жүргізілді. Алынған T2WI, DWI реттілігі бір-бірімен және қуық асты безінің анатомиялық құрылымына сәйкес салыстырылды. Қуық асты безінің қатерлі ісігінің күдікті жерлері қызығушылық аймақтары ретінде (ROI) белгіленді, олар үшін өлшенетін диффузия коэф-*

фициенті (ADC) есептелді. Қуық асты безінің қатерлі ісігінің болуы немесе болмауы ультрадыбыстық бақылаудағы 12 нүктелі трансректалды биопсияның көмегімен расталды.

Нәтижелері: *сандық өлшемдерді талдау кезінде, қалыпты тінмен салыстырғанда, ADC орталық бездегі қатерлі ісік (өтпелі аймақ және орталық аймақ) үшін төмен мәндерді көрсетті – 0,610±0,157×10^{-3} мм^2/с, p=0,0001 және перифериялық аймақтағы ісік үшін – 0,651±0,228×10^{-3} мм^2/с, p=0.0004. Сезімталдықтың ең жоғары мәні (87,5%) ADC орталық без үшін, ал төменгі мән ADC перифериялық аймақ үшін 75% болатыны анықталды. Ең жоғары ерекшелік мәні (90,9%) ADC перифериялық аймақ, ал төменгі мән ADC орталық без – 84,1% болды.*

Қорытынды: *DWI – қуық асты безінің қатерлі ісігін анықтау, локализациялау, қуық асты безінің қатерлі ісігінің сапалық (визуалды) және сандық бағалауын қамтамасыз ететін пайдалы инвазивті емес әдіс.*

Түйінді сөздер: *мультипараметрлік магнитті-резонанстық томография, трансректалды ультрадыбыстық зерттеу, диффузиялық өлшенген бейнелеу (DWI).*

АННОТАЦИЯ

ВОЗМОЖНОСТИ DWI В ДИАГНОСТИКЕ РАКА ПРЕДСТАТЕЛЬНОЙ ЖЕЛЕЗЫ

К.Е. Каракойшин[1], Ж.Ж. Жолдыбай[1], А.С. Айнакулова[1], Д.К. Толешбаев[1], Г.М. Мухит[1], Е. Айсербай[1]

[1]НАО «Казахский Национальный Медицинский Университет имени С.Д. Асфендиярова», Алматы, Республика Казахстан

Актуальность: *Рак предстательной железы (РПЖ) является одной из главных причин смертности мужчин от онкологических заболеваний во всем мире. Трансректальная биопсия предстательной железы (ПЖ) под контролем ультразвукового исследования (ТРУЗИ) является важнейшим диагностическим этапом, без которого невозможно поставить окончательный диагноз. Несмотря на это, биопсия ПЖ под контролем ТРУЗИ имеет высокий уровень ложно-отрицательных результатов и часто сопровождается различными клиническими осложнениями. Мультипараметрическая МРТ (мпМРТ) в настоящее время активно применяется в повседневной урологической и онкологической практике. Одним из элементов мультипараметрической МРТ является диффузионно-взвешенная визуализация (DWI), которая успешно используется в выявлении и локализации клинически значимого РПЖ.*

Цель исследования *– оценить возможности DWI в диагностике рака предстательной железы.*

Методы: *52 пациентам в возрасте 48-86 лет с подозрением на РПЖ была проведена мпМРТ. DWI последовательности, полученные при помощи Т2-взвешенной визуализации (T2WI), были сопоставлены между собой и сравнены с анатомическим строением ПЖ. Подозрительные на рак участки ПЖ были отмечены как области интереса, для которых рассчитывали измеряемый коэффициент диффузии (apparent diffusion coefficient, ADC). Наличие или отсутствие РПЖ было подтверждено путем проведения 12-точечной биопсии под контролем ТРУЗИ.*

Результаты: *При анализе количественных измерений ADC показала низкие значения при раке в центральной железе (переходная зона и центральная зона) – 0,610±0,157×10^{-3} мм^2/с, p=0,0001 и при раке в периферической зоне – 0,651±0,228×10^{-3} мм^2/с, p=0,0004, по сравнению с нормальной тканью. Установлено, что наибольшее значение чувствительности (87,5%) характерно для ADC центральной железы, а меньшее значение для ADC периферической зоны – 75%. Наибольшее значение специфичности (90,9%) наблюдалось у ADC периферической зоны, а меньшее значение у ADC центральной железы – 84,1%.*

Заключение: *DWI – эффективный неинвазивный метод диагностики и локализации РПЖ, обеспечивающий качественную (визуальную) и количественную оценку РПЖ.*

Ключевые слова: *рак предстательной железы (РПЖ), мультипараметрическая магнитно-резонансная томография (мпМРТ), трансректальное ультразвуковое исследование (ТРУЗИ), диффузионно-взвешенная визуализация (DWI).*

Transparency of the study: *Authors take full responsibility for the content of this manuscript.*
Conflict of interest: *Authors declare no conflict of interest.*
Financing: *Authors declare no financing of the study.*
Authors' input: *contribution to the study concept – Zholdybai Zh.Zh., Ainakulova A.S., Toleshbayev D.K., Muhit G.M., Aiserbai E.; study design – Ainakulova A.S., Zholdybai Zh.Zh; execution of the study – Karakoishin K.E.; interpretation of the study – Karakoishin K.E., Zholdybai Zh.Zh.; preparation of the manuscript – Karakoishin K.E., Zholdybai Zh.Zh.*

Authors' data:
Karakoishin Kanat Yesenkululy (corresponding author) – PhD student, Assistant at Visual Diagnostics Department, “Asfendiyarov Kazakh National Medical University” NCJSC, tel. +77475168571, e-mail: kanat.karakoishin@yandex.ru, ORCID ID: 0000-0003-4013-4487;
Zholdybai Zhamilya Zholdybayevna – Doctor of Medical Sciences, Professor, Head of Visual Diagnostics Department, “Asfendiyarov Kazakh National Medical University” NCJSC, tel. +77772101612, e-mail: joldybay.j@gmail.com, ORCID ID: 0000-0003-0553-9016;
Ainakulova Akmaral Serikovna – PhD, Assistant at Visual Diagnostics Department, “Asfendiyarov Kazakh National Medical University” NCJSC, tel. +77017242429, e-mail: ar89@list.ru, ORCID ID: 0000-0003-1773-5145;
Toleshbayev Dias Kairatovich – PhD candidate, Assistant at Visual Diagnostics Department, “Asfendiyarov Kazakh National Medical University” NCJSC, tel. +77475574025, e-mail: d1sk.88@mail.ru, ORCID ID: 0000-0002-7010-8776;
Muhit Gauhar Muhitkyzy – resident at “Asfendiyarov Kazakh National Medical University” NCJSC, tel. +77088419645, e-mail: gaumuhitkyzy@gmail.com, ORCID ID: 0009-0002-0994-975X;
Aiserbai Yernar – resident at “Asfendiyarov Kazakh National Medical University” NCJSC, tel. +77769866617, e-mail: ernargumi005@gmail.com, ORCID ID: 0009-0008-7639-0953.

Address for correspondence: Karakoishin K.E., mcd. Daraboz, 43, apt. 53, Almaty, 050038, the Republic of Kazakhstan.